Proceedings of the Institute of Acoustics

DYNAMIC SIMULATION AND VIBRATION CONTROL OF FLEXIBLE MANIPULATOR SYSTEMS

M O Tokhi and A K M Azad

Department of Automatic Control and Systems Engineering, The University of Sheffield, UK.

1. INTRODUCTION

The increasing demands at process automation and control in various applications have necessitated the employment of robotics technology in recent years. The performance demands including faster system response, lower energy consumption, requiring relatively small actuators, reduced non-linearity due to elimination of gearing, less overall cost, on the other hand, has motivated the utilisation of flexible manipulator systems. The flexible nature of such manipulators, however, lead to an oscillatory behaviour in the form of undesirable structural vibrations in the system [1]. Moreover, to compensate for flexure effects and thus yield robust control, the design focuses primarily on non-collocated controllers [2,3]. In this context, it is important initially to recognise the flexible nature of the manipulator and construct a mathematical model of the system that accounts for the interactions with actuators and payload.

This paper presents the development of a dynamic simulation algorithm and a control mechanism for flexible manipulator systems to achieve a target displacement with reduced elastic deflections (vibration). A single-link flexible manipulator with its movement confined to a two-dimensional space coordinate system is considered. A finite dimensional simulation of the manipulator is developed through discretisation, both in time and space co-ordinates using a finite difference (FD) approximation to the governing dynamic equation of the structure. The algorithm is implemented on an i860 digital signal processing (DSP) device in real-time and its performance assessed. Two types of output feedback controllers featuring a collocated and a hybrid collocated/non-collocated control mechanism are developed. The collocated control mechanism incorporates hub angle and hub velocity feedback through a proportional and derivative (PD) arrangement. The hybrid controller incorporates, additionally, end-point acceleration feedback with the joint-based PD controller. The control mechanisms thus developed are implemented and their performance assessed.

2. DYNAMIC SIMULATION

A schematic representation of a single-link manipulator system is shown in Figure 1, where a manipulator of a moment of inertia I_b, hub inertia I_h, a linear mass density ρ and a length l is considered. A payload of mass M_p and inertia I_p are incorporated at the free-end of the manipulator. A control torque $\tau(t)$ as a function of time t is applied at the hub (point O) of the manipulator by an actuator motor causing the manipulator to move in the PQ-plane. The angular displacement of the manipulator from a reference position (OP-axis) is denoted by $\theta(t)$. x represents the distance along the beam length from the hub position and u represents the elastic deflection of the beam (measured from line Ox) at a point x along its length. It is assumed that the height of the manipulator is substantially greater than its width (thickness) so that its vibration is dominantly confined to the PQ-plane (horizontal direction). Moreover, shear deformation and rotary inertia effects are assumed to be negligible and thus are ignored.

It follows from Figure 1 that the displacement $y(x,t)$ of a point along the beam at a distance x from the hub at time t is a function of both the rigid body motion $\theta(t)$ and the elastic deflection $u(x,t)$;

$$y(x,t) = x\theta(t) + u(x,t) \tag{1}$$

Obtaining the energies associated with this system and using the Hamilton's extended principle, [4], yields the dynamic equation of motion of the manipulator as

$$EI\frac{\partial^4 y}{\partial x^4} + \rho\frac{\partial^2 y}{\partial t^2} = \tau(x,t) \tag{2}$$

with the associated boundary conditions as

$$\begin{aligned} y(0,t) &= 0 \quad , \quad I_p\frac{\partial^3 y(0,t)}{\partial t^2 \partial x} + EI\frac{\partial^2 y(0,t)}{\partial x^2} = \tau(t) \\ I_p\frac{\partial^3 y(l,t)}{\partial t^2 \partial x} + EI\frac{\partial^2 y(l,t)}{\partial x^2} &= 0 \quad , \quad M_p\frac{\partial^2 y(l,t)}{\partial x^2} + EI\frac{\partial^3 y(l,t)}{\partial x^3} = 0 \end{aligned} \tag{3}$$

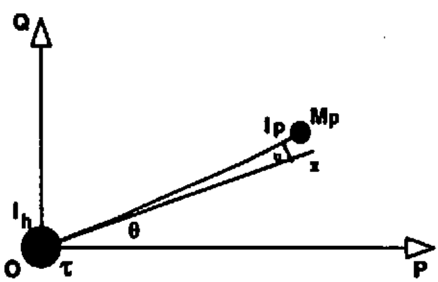

Figure 1: Schematic representation of the flexible manipulator system.

and initial conditions as

$$y(x,0)=0 \quad \text{and} \quad \frac{\partial y(x,0)}{\partial t}=0 \tag{4}$$

where E, I and I_p represent the Young's modulus, second moment of inertia and payload inertia of the beam respectively. The fourth-order PDE in equation (2) with the associated boundary and initial conditions in equations (3) and (4) give the dynamic equation describing the motion of the flexible manipulator.

A finite dimensional simulation of the flexible manipulator system is developed through discretisation both in time and space coordinates using an FD approximation to the PDE in equation (2). The proposed algorithm allows the inclusion of a distributed actuator and sensor term in the PDE and modification of boundary conditions. A set of difference equations defined by the central difference quotients of the FD method, [5], are obtained to replace the PDE. The manipulator length and movement time are each divided into suitable number of sections of equal length represented by Δx ($x = i\Delta x$) and Δt ($t = j\Delta t$), where i and j are non-negative integer numbers, respectively. This yields the displacement $y_{i,j+1}$ of grid point i at time instant $j+1$ as [6]

$$y_{i,j+1} = -c\left[y_{i-2,j} + y_{i+2,j}\right] + b\left[y_{i-1,j} + y_{i+1,j}\right] + a y_{i,j} - y_{i,j-1} + \frac{\Delta t^2}{\rho}\tau(i,j) \tag{5}$$

where, $a = 2 - \dfrac{6\Delta t^2 EI}{\rho h^4}$, $b = \dfrac{4\Delta t^2 EI}{\rho h^4}$ and $c = \dfrac{\Delta t^2 EI}{\rho h^4}$. Equation (5) gives the displacement of section i of the manipulator at time step $j+1$. This is the required relation for the simulation algorithm that can be implemented on a digital processor easily.

It follows from equation (5) that, to obtain the displacements $y_{1,j+1}$, $y_{n-1,j+1}$ and $y_{n,j+1}$ the displacements of the fictitious points $y_{-1,j}$, $y_{n+1,j}$ and $y_{n+2,j}$ are required. The estimation of these displacements are obtained using the boundary and initial conditions related to equation (2) The stability of the algorithm can be examined by ensuring that the iterative scheme described in equation (5) converges to a solution. The necessary and sufficient condition for stability satisfying this convergence requirement is given by $0 \le c \le 0.25$, [7].

The simulation algorithm thus developed was implemented on an i860 DSP device and its performance was assessed. The flexible motion of the manipulator as superimposed on the rigid body motion is shown in Figure 2. The corresponding second and higher flexible modes are shown in Figure 3. A comparison of these two diagrams reveals that the magnitude of vibration at the second mode is about ten times smaller than that at the first mode. Investigations were carried out to observe the effect of a payload on the manipulator response. It was found that the addition of the payload results in a reduction in the total end-point displacement of the manipulator. Moreover, the frequency of vibration is reduced and at the same time the level of vibration is increased as a result of adding a payload.

3. CONTROL OF THE MANIPULATOR

Investigations have shown that the only non-collocated sensor/actuator pair that has successfully been employed previously includes the motor torque with either the beam strain or global/local end-point position [3]. However, practical realisation of both methods have associated short term and long term drawbacks. To tackle these associated problems it is proposed here to devise a control strategy that uses both the collocated (hub angle and hub velocity) and non-collocated (end-point acceleration) feedback. In this context a collocated controller and a combined collocated and non-collocated controller are developed and their performances assessed.

3.1. Joint based Collocated Controller

A common strategy in the control of manipulator systems involves the utilisation of proportional and derivative (PD) feedback of collocated sensor signals. A block diagram of the PD controller is shown in Figure 4, where K_p and K_v are the proportional and derivative gains, θ represents hub angle, $\dot{\theta}$ represents hub velocity, R_f is the reference hub angle and A_c is the gain of the motor amplifier. To design the PD controller a linear state-space model of the manipulator was

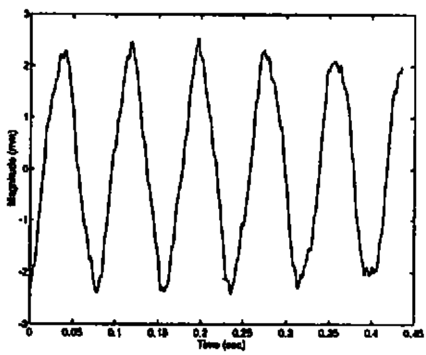

Figure 2: Flexible end-point motion.

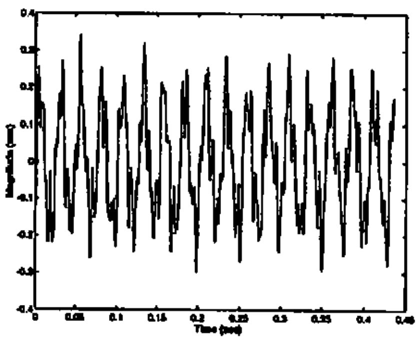

Figure 3: Second and all higher modes at end-point.

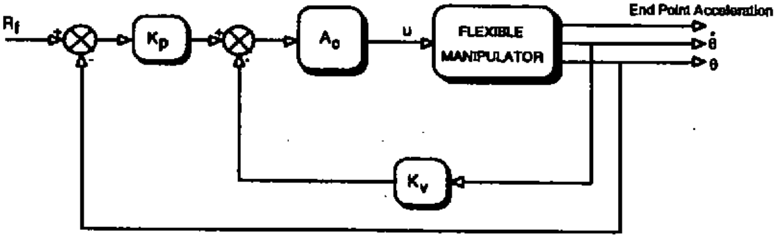

Figure 4: Flexible manipulator system with joint based collocated controller.

obtained by linearising the equations of motion of the system. The first two flexible modes of the manipulator were assumed to be dominantly significant.

The control signal $u(s)$ in Figure 4 can thus be written as

$$u(s) = A_c\left[K_p\left(R_f(s) - \theta(s)\right) - K_v\dot{\theta}\right]$$

where, s is the Laplace variable. The closed-loop system transfer function is, therefore, obtained as

$$\frac{\theta(s)}{R_f(s)} = \frac{K_p H(s) A_c}{1 + K_v\left(s + K_p/K_v\right)H(s)A_c}$$

where, $H(s)$ is the open-loop transfer function from the input torque, u, to hub angle, given by

$$H(s) = C(sI - A)^{-1}B \tag{6}$$

where, A, B, and C are the characteristic matrix, input matrix and output matrix of the system respectively. Thus, the closed-loop poles of the system are obtained from the closed-loop characteristic equation represented by

$$1 + K_v(s + Z)H(s)A_c = 0$$

where, $Z = K_p/K_v$ represents the compensator zero which determines the control performance and characterises the shape of root-locus of the closed-loop system. It is well known that theoretically any choice of the gains K_p and K_v assures the stability of the system [8]. However, in practice this is no longer valid. This is due to the uncontrolled dynamics of the flexible manipulator, actuator and sensors as well as delays caused by measuring and sampling of feedback signals.

To investigate the performance of the PD controller the response of the system was studied in comparison to its open-loop response for torque and energy inputs at the hub. For the open-loop system the bang-bang torque input shown in Figure 5 is used for minimum time movement. A step reference input is provided to the system with PD feedback control. Figure 6 shows the end-point displacement for the system in open-loop and closed loop control. As noted, with the PD control, the end-point settles within 1.9 seconds. In open-loop, however, it oscillates for much longer time (2 seconds). The end-point deflection as function of time is shown in Figure 7. It is clear from this diagram that the magnitude of end-point oscillation is much higher for the open-loop system than the PD control. Moreover, with PD control, oscillations disappear quickly and the system smoothly comes to rest at about 1.8 secs, whereas, for the open-loop system the response remains oscillatory to about 4 seconds.

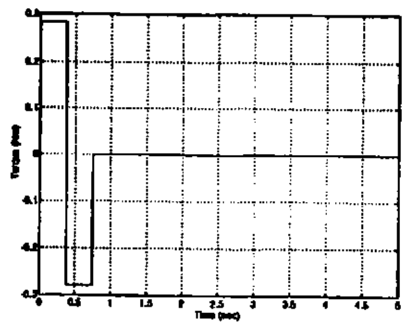

Figure 5: Open-loop torque input.

Moreover, it was found that the input energy required for the PD controlled system is of the order of five times less than that of the open-loop system. These results demonstrate the significant improvement in system performance with PD control using hub angle and hub velocity feedback, as compared to the open-loop system.

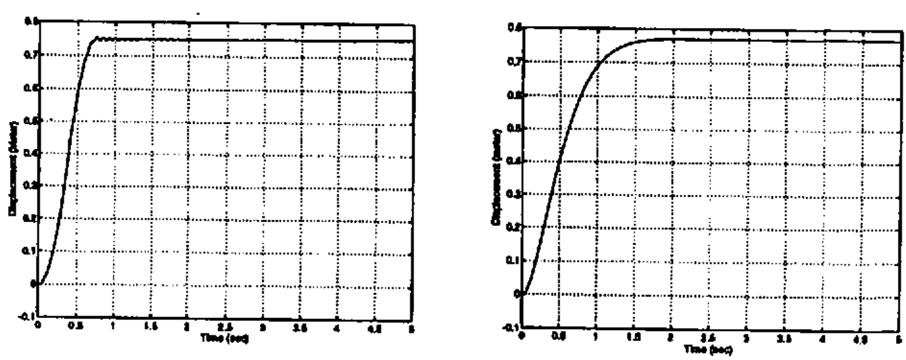

(a) Open-loop bang-bang.

(b) PD Controlled.

Figure 6: End-point displacement of the flexible manipulator.

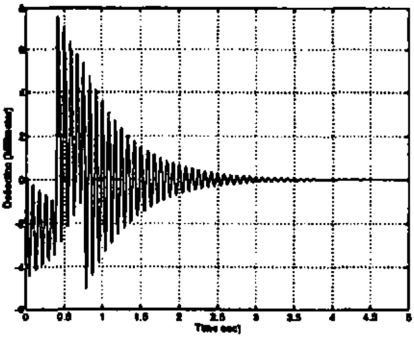

(a) Open-loop bang-bang.

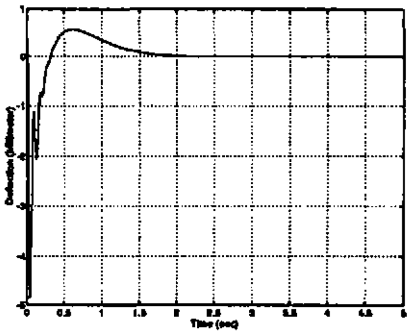

(b) PD Controlled.

Figure 7: End-point elastic movement of the flexible manipulator.

3.2. Hybrid collocated and non-collocated controller

A block diagram of the hybrid collocated and non-collocated control structure is shown in Figure 8. The controller design utilises end-point acceleration feedback through a static feedback gain. Moreover, the hub angle and hub velocity feedback are also used in a PD configuration for controlling the rigid body motion of the manipulator. The control structure, thus, comprises of two feedback loops; one using the filtered end-point acceleration as input to a control law, and the other using the filtered hub angle and hub velocity as input to a separate control law. These two loops are then summed to give a command motor input voltage, which produces a torque.

Consider first the rigid body control loop, in which the hub angle θ and hub velocity $\dot{\theta}$ are the output variables. The open-loop transfer function could be obtained from equation (6). To design the controller in this loop a low-pass filter is required for both θ and $\dot{\theta}$ so that the flexible modes are attenuated before reaching the controller input. The appropriate proportional and derivative gains are determined from a root locus analysis, producing 40dB gain margin and ample phase margin.

The flexible motion of the manipulator is controlled by using the end-point acceleration feedback through a PID controller. The transfer function of the flexible manipulator with end-point acceleration as output is obtained from equation (6). The end-point acceleration is fed back through a low-pass filter with a cut-off frequency of 40Hz. The values of proportional, derivative and integral gains are adjusted using the Ziegler-Nichols procedure [9]. Figures 9 and 10 show the end-point displacement and elastic movement of the manipulator using this controller.

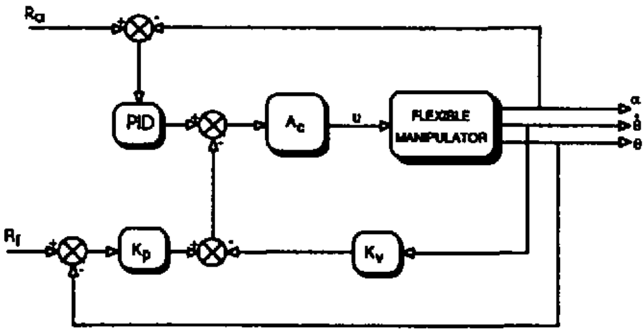

Figure 8: Block diagram of the hybrid collocated and non-collocated controller.

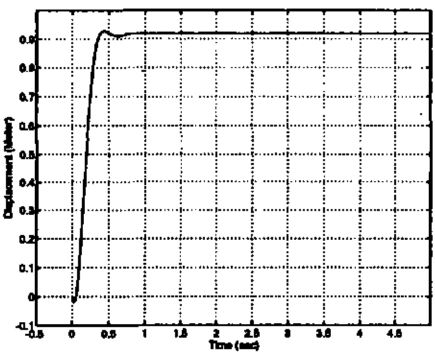

Figure 9: End-point displacement.

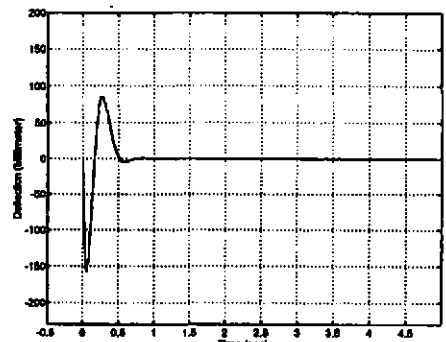

Figure 10: End-point elastic movement.

It is seen that the target displacement is achieved in 0.5 sec; this is three times faster than that with the PD controlled system, Figure 6(a). A comparison of Figures 10 and 7(a) shows that the elastic deflection settles down much quicker in the case of the hybrid controller. However, the amplitude of elastic deflection is relatively higher in this case. This was further confirmed by the peak input energy required; which is higher than that for the PD controlled system.

The use of acceleration feedback for rigid or flexible manipulator control has intuitive appeal from an engineering design viewpoint. However, the primary advantage of this is that sensing for control implementations is done with structure mounted devices so that camera position or field of view are not the issues of concern, as common in previous methods. This, from a practical viewpoint, is easier and cheaper to implement. Moreover, application of this strategy to multi-link flexible manipulators, to utilise these advantages to a greater extent, will be favoured.

4. CONCLUSION

A simulation algorithm for a flexible manipulator system has been developed and implemented using finite difference methods. It has been demonstrated that the level of vibration as well as the angular displacement of the manipulator decrease with the addition of a payload. Moreover, for a given value of c, an increase in the number of grid points along the length of the manipulator results in a decrease in the value of Δt. This, in turn, leads to an enhancement in the detailed description of the manipulator movement. However, such an enhancement is achieved at the expense of increased computational burden on the processor which could, specially, be a major issue of concern in real-time applications. A payload checking facility has been incorporated within the algorithm, which allows avoiding un-necessary repetitive calculations and hence making the simulation time relatively shorter.

Two controller design strategies have been presented. A hub angle and hub velocity based collocated controller has been developed and its performance has been assessed in comparison to a bang-bang input torque for similar scale of movement. The results show that considerable improvement in system performance is achieved with PD controlled system. A control strategy based on hub angle and hub velocity feedback for rigid body motion control and end-point acceleration feedback for flexible motion control has also been developed. Results of such a strategy demonstrate that the system performance improves significantly. The advantages of acceleration feedback include ease of implementation, raggedness, relatively low cost, and allowing the use of structure mounted sensing. The latter is extremely important for extensions of this work to multi-link systems where the use of e.g. cameras and other optical measurement systems could be impractical.

5. REFERENCES

[1] M J Balas, . 'Feedback Control of Flexible Systems', IEEE Transaction on Automatic Control, AC-23 p.673-679 (1978)

[2] R H Cannon & E Schmitz, 'Initial Experiments on the End-Point Control of a Flexible One-Link Robot', The Int. Journal of Robotics Research, 3 p.62-75 (1984)

[3] F Harishima & T Ueshiba, 'Adaptive Control of Flexible Arm using end-point position sensing', Proceedings of Japan-USA Symposium of Flexible Automation, 14-18 July, Osaka, Japan, p.225-229 (1986)

[4] L Meirovitch, 'Analytical Methods in Vibrations', The Macmillan Company, New York (1967)

[5] L Lapidus, 'Numerical Solution of Partial Differential Equations in Science and Engineering', John Wiley and Sons, New York (1982)

[6] M O Tokhi, A K M Azad and M A Hossain, 'Simulation of a flexible manipulator system under practical constraints', Proceedings of SIMTEC-93: International simulation Technology Conference, 07-10 November, San Francisco, p. 45-50 (1993)

[7] P K Kourmoulis, 'Parallel Processing in the Simulation and Control of Flexible Beam Structure', Ph.D. Thesis, University of Sheffield, Department of Automatic Control and Systems Engineering (1990)

[8] W B Gravarter, 'Basic Relations for Control of Flexible Vehicles', AIAA Journal, 8, p.666-672 (1970)

[9] K Warwick, 'Control System: An Introduction', Prentice-Hall Inc., UK (1989)